Article

Development of a Targeted SN-38-Conjugate for the Treatment of Glioblastoma

Perpetue Bataille Backer, Tayo Alex Adekiya, Yushin Kim, Terry-Elinor R. Reid, Michael Thomas, and Simeon K. Adesina*
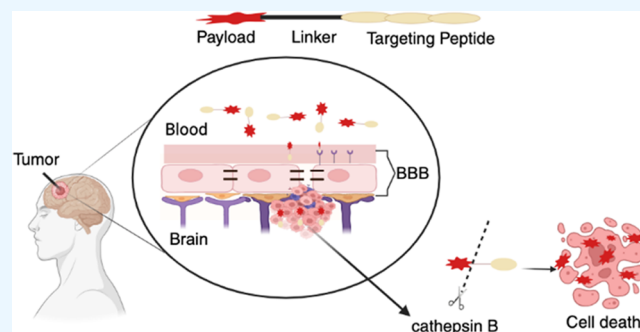
Read Online

ACCESS | Metrics & More | Article Recommendations | Supporting Information

ABSTRACT: Glioblastoma (GBM) is the most aggressive and fatal brain tumor, with approximately 10,000 people diagnosed every year in the United States alone. The typical survival period for individuals with glioblastoma ranges from 12 to 18 months, with significant recurrence rates. Common therapeutic modalities for brain tumors are chemotherapy and radiotherapy. The main challenges with chemotherapy for the treatment of glioblastoma are high toxicity, poor selectivity, and limited accumulation of therapeutic anticancer agents in brain tumors as a result of the presence of the blood−brain barrier. To overcome these challenges, researchers have explored strategies involving the combination of targeting peptides possessing a specific affinity for overexpressed

cell-surface receptors with conventional chemotherapy agents via the prodrug approach. This approach results in the creation of peptide drug conjugates (PDCs), which facilitate traversal across the blood−brain barrier (BBB), enable preferential accumulation of chemotherapy within the neoplastic microenvironment, and selectively target cancerous cells. This approach increases accumulation in tumors, thereby improving therapeutic efficiency and minimizing toxicity. Leveraging the affinity of the HAIYPRH (T7) peptide for the transferrin receptor (TfR) overexpressed on the blood−brain barrier and glioma cells, a novel T7-SN-38 peptide drug conjugate was developed. The T7-SN-38 peptide drug conjugate demonstrates about a 2-fold reduction in glide score (binding affinity) compared to T7 while maintaining a comparable orientation within the TfR target site using Schrödinger-2022−3 Maestro 13.3 for ligand preparation and Glide SP-Peptide docking. Additionally, SN-38 extends into a solvent-accessible region, enhancing its susceptibility to protease hydrolysis at the cathepsin B (Cat B) cleavable site. The SN-38-ether-peptide drug conjugate displayed high stability in buffer at physiological pH, and cleavage of the conjugate to release free cytotoxic SN-38 was observed in the presence of exogenous cathepsin B. The synthesized peptide drug conjugate exhibited potent cytotoxic activities in cellular models of glioblastoma in vitro. In addition, blocking transferrin receptors using the free T7 peptide resulted in a notable inhibition of cytotoxicity of the conjugate, which was reversed when exogenous cathepsin B was added to cells. This work demonstrates the potential for targeted drug delivery to the brain in the treatment of glioblastoma using the transferrin receptor-targeted T7-SN-38 conjugate.

INTRODUCTION

Glioblastoma (GBM) is one of the most challenging forms of cancer to treat, with a median survival period of around 16 months. It has a survival rate of less than 5.8% at the 5-year mark and a recurrence rate of 90%.[1−3] The primary clinical approach for GBM involves maximal surgical resection, followed by radiotherapy with concomitant Temozolomide and maintenance over time with Temozolomide (TMZ) chemotherapy.[4,5] Nevertheless, complete eradication of the brain tumor is often not feasible due to the inherent resistance of glioblastoma cells, the invasive nature of the tumor cell growth within tissues, and the specific location where the tumor develops.[2,4] Unlike peripheral tumors, brain tumors present distinct challenges for treatment, primarily due to the presence of the blood−brain barrier (BBB), which restricts the

penetration and accumulation of chemotherapeutic agents to the tumor site.[4,6,9]

The BBB, serving as both a physical and biological barrier, plays a pivotal role in safeguarding the central nervous system (CNS).[10,11] The BBB operates with a tightly controlled transport mechanism.[10,12] Although these characteristics are crucial for maintaining the optimal neuronal environment, they limit the effectiveness of most chemotherapeutic agents in
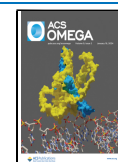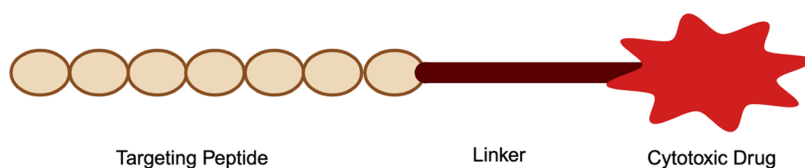
Figure 1. General structure of a targeted peptide drug conjugate. Created with BioRender.com.

treating glioblastoma.[4,11] Thus, high drug dosages are required in order to reach therapeutic levels in the tumor. In addition, resistance to chemotherapy and undesired side effects stemming from nonspecific interactions between the anticancer agent and healthy cells are other challenges associated with the treatment of glioblastoma.[7] However, in high-grade gliomas (glioblastoma is a grade 4 glioma), the integrity of the BBB is oftentimes compromised by a series of alterations caused by the rapid proliferation of the tumor cells leading to the emergence of a microenvironment that is distinct from the normal brain tissues, termed the blood−brain tumor barrier (BBTB).[7,8,12]

A distinctive characteristic of the BBB is the expression of several receptors, including those associated with angiogenesis, like vascular endothelial growth factor receptor (VEGFR), platelet-derived growth factor receptor (PDGFR), and epidermal growth factor receptor (EGFR), as well as integrin receptors, low-density lipoprotein receptors (LDLR), and transferrin receptors (TfRs).[13] The transferrin receptor plays a crucial role in facilitating the transfer of iron into the brain parenchyma, ensuring the maintenance of iron balance, which is significant for metabolic processes, neural conductivity, and, consequently, the normal functioning of the brain.[14] The transferrin receptor presents itself as a fascinating and distinctive target in the treatment of glioblastoma due to its exclusive expression on the endothelial cells of brain capillaries, contrasting with its absence on the endothelial cells lining blood vessels in other tissues.[14−16] Additionally, it has been reported that the expression of TfR on GBM cells is up to 100-fold higher compared to healthy cells.[17,18] This is attributed to the escalated demand for iron by malignant cells to support their rapid proliferation.[9] Thus, the TfR is a promising target for site-specific drug delivery and intratumoral accumulation for the treatment of GBM using receptor-mediated transcytosis (RMT).[5,12,17,19]

Among the various targeting ligands available for TfR, Transferrin (Tf) has emerged as an appealing option for delivering drugs specifically to glioblastoma.[13,20,21] Tf employs RMT to facilitate the transfer of iron-bound transferrin from the luminal side to the basolateral side of the brain. However, the presence of high concentrations of endogenous Tf competitively inhibits Tf-modified delivery systems. Therefore, alternative ligands with similar affinity for TfR were developed.[13]

The T7 peptide, with the sequence His-Ala-Ile-Tyr-Pro-Arg-His (HAIYPRH), is a heptapeptide that specifically targets TfR on the BBB/BBTB and on the brain tumor cells.[5,16,20] Its binding affinity is comparable to that of Tf.[13,20] Furthermore, the T7 binding site on TfR is reported to be different from that of Tf, avoiding interference with endogenous Tf. The cellular uptake of T7-conjugated drug delivery systems was also found to be accelerated when endogenous Tf is bound to TfR, highlighting T7 as a promising carrier strategy for drug delivery systems targeting glioblastoma (GBM).[13,20]

The conjugation of T7 peptide to various nanocarriers for targeted delivery to GBM has been reported.[18,22−26] Of these strategies, targeted conjugates using the prodrug approach offer distinct advantages, such as controllable and predictable drug release, when compared to vesicular systems that release the drug payload via diffusion. Antibody-drug conjugates (ADCs) have been approved by the US FDA for the treatments of cancers;[27] however, their large size and other issues such as immunogenicity and stability are challenges associated with their use.[27,28] Recently, researchers have reported that peptide drug conjugates (PDCs) are devoid of the challenges associated with ADCs. They are small, nonimmunogenic, and relatively more stable than antibodies.[28]

Figure 1 illustrates the components of a PDC. A PDC consists of a peptide ligand with affinity for receptors found on the target cells, a linker that connects the drug payload to the targeting peptide, and a toxin or the drug payload.[29,30] The linker may be cleavable, thereby serving as the mechanism of drug release. This characteristic is important for controlling drug release for specific drug delivery to the target site while minimizing drug impact on healthy tissues.[31] The use of protease-cleavable linkers, frequently taking the form of distinct peptide sequences, is designed to undergo cleavage solely upon recognition by the proteases that are upregulated within the boundaries of the tumor microenvironment.[31,32] An example of such protease overexpressed in tumors is cathepsin B (Cat B), a lysosomal protease, which is secreted into the tumor microenvironment and aids the spread of cancer cells by degrading components of the extracellular matrix (ECM).[33] Cathepsin B is overexpressed in various tumor types, including glioblastoma cells.[32,34] The valine-alanine (VA) dipeptide is a cathepsin B recognition sequence that has demonstrated stability in serum, and conjugates containing the sequence are stable in plasma until it accumulates in the tumor where cathepsin B is overexpressed.[35] The protease recognizes and binds to the VA sequence, initiating a chemical reaction that leads to the cleavage of the linker after alanine.[36,37] The cleavage of the VA linker results in the release of the drug molecule from the conjugate. This allows the drug to become active and exert its therapeutic effects at the intended site of action.

7-Ethyl-10-hydroxycamptothecin, also known as SN-38, is an active metabolite of irinotecan, which has been reported to demonstrate 100−1000 times greater potency compared to irinotecan and displays potent inhibitory effects against DNA topoisomerase I.[38,39] SN-38 is an effective cytotoxic agent against primary and recurrent glioma cells.[40,41] However, it is lipophilic, highly toxic when administered intravenously, and unstable in the physiological environment, which limits its clinical application.[42] Therefore, a peptide drug conjugate is ideal for improving SN-38's low circulation half-life, solubility, and cytotoxicity profile.

In the present work, the cytotoxic drug SN-38 is coupled to the tumor-targeting T7 peptide via a cathepsin B cleavable VA peptide linker. This ensures that the drug remains covalently
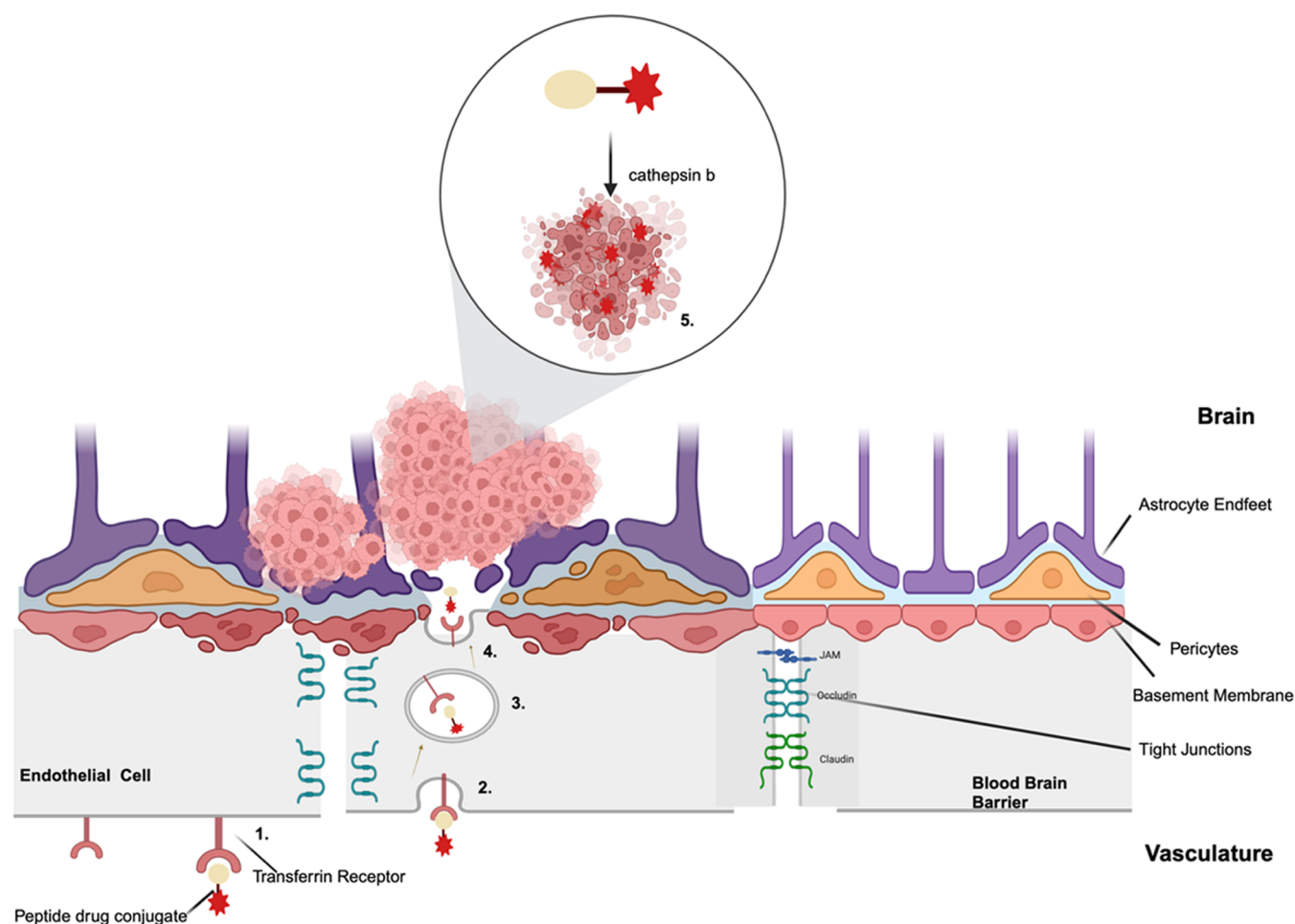
Figure 2. Receptor-mediated transcytosis for drug delivery across the BBB. (**1**) The transferrin receptor targeting peptide (T7) binds to transferrin receptors on the BBB. (**2**) T7-SN-38 forms a receptor–ligand complex on the cell membrane, and the cell membrane begins to invaginate, creating a small region called the clathrin-coated pit. (**3**) The clathrin-coated pit eventually pinches off from the cell membrane, forming a vesicle known as a clathrin-coated vesicle or endosome, which contains the T7-SN-38 conjugate. (**4**) Release of T7-SN-38 to the tumor site followed by binding to transferrin receptors overexpressed on glioblastoma cells. (**5**) Cat B cleavage of the VA linker leads to the liberation of SN-38 from the complex. This activates the cytotoxic drug in the tumor microenvironment. Created with BioRender.com.

bound until it reaches the intended site of action, where Cat B is overexpressed (Figure 2) to release the drug. Within this framework, our research pursuits entail the synthesis and characterization of a T7-SN-38-targeted drug conjugate using strain-promoted azide-alkyne cycloaddition (SPAAC). Our investigation extended to evaluating the cellular uptake and assessing the cytotoxicity of the drug conjugate in U87MG glioblastoma cells.

EXPERIMENTAL SECTION

Materials. All reagents listed below were obtained from commercial sources and used without further purification. H-His (Trt)-2-Cl-Trt resin and H-Val-2-Cl-Trt resin were purchased from AAPPTEC (Louisville, KY). Boc-L-alanine, Fmoc-L-alanine, N^{α}-Fmoc-N^{ω}-(2,2,4,6,7-pentamethyldihydro-benzofuran-5-sulfonyl)-L-arginine, N^{im}-Trityl-L-histidine tert-butyl ester hydrochloride, Fmoc-L-isoleucine, Fmoc-O-tert-butyl-L-tyrosine, Fmoc-L-proline, Fmoc-6-aminohexanoic acid, 4-aminobenzyl alcohol (PABA), O-(7-azabenzotriazol-1-yl)-N,N,N′,N′-tetramethyluronium hexafluorophosphate (HATU),N-ethoxycarbonyl-2-ethoxy-1,2-dihydroquinoline-(EEDQ),N,N′-diisopropylethylamine (DIPEA), trifluoroacetic acid (TFA), and piperidine were purchased from Chem Impex

(Wood Dale, IL). 7-Ethyl-10-hydroxycamptothecin (SN-38) was purchased from Biosynth (San Diego, CA). N,N-dimethylformamide (DMF), dichloromethane (DCM), methanol (MeOH), tetrahydrofuran (THF), acetonitrile (ACN), ethyl acetate (EtOAc), hexane, triisopropylsilane (TIPS), phosphorus tribromide, diethyl ether (Et_2O), silica gel, 18-crown-6, and potassium carbonate were purchased from Sigma-Aldrich (Burlington, MA). N_3-PEG$_4$-acid, Fmoc-N-amido-PEG$_3$-acid, and DBCO-C$_6$-acid were purchased from BroadPharm (San Diego, CA).

Peptide Molecular Docking. The protein crystal structure of TfR (PDB code: 3S9N) was used to conduct molecular docking binding predictions.[43] The designed peptides were subsequently imported into Schrödinger-2022−3 Maestro 13.3 for ligand preparation and Glide SP-Peptide docking that has been optimized to enhance peptide sampling and scoring.[44,45] Using Maestro LigPrep, the peptide structures were preprocessed for docking: OPLS4 forcefields were generated, and ionization states of the peptides were generated at pH 7.4 ± 2.0 using the pK_a predicting module Epik. Ligands were preprocessed with the ConfGen algorithm of Maestro, which generates the low-energy conformations for rigid-body docking. Low-energy conformations and stereo-
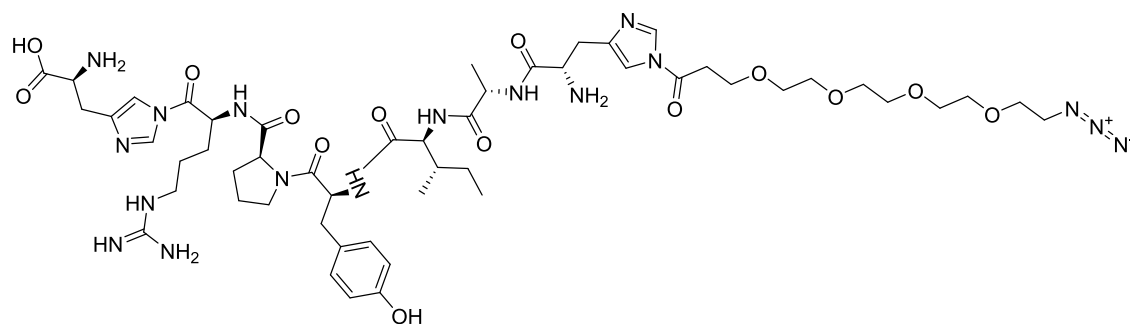
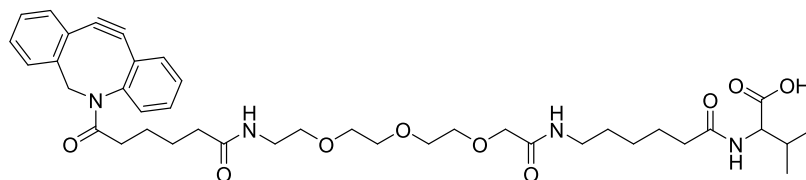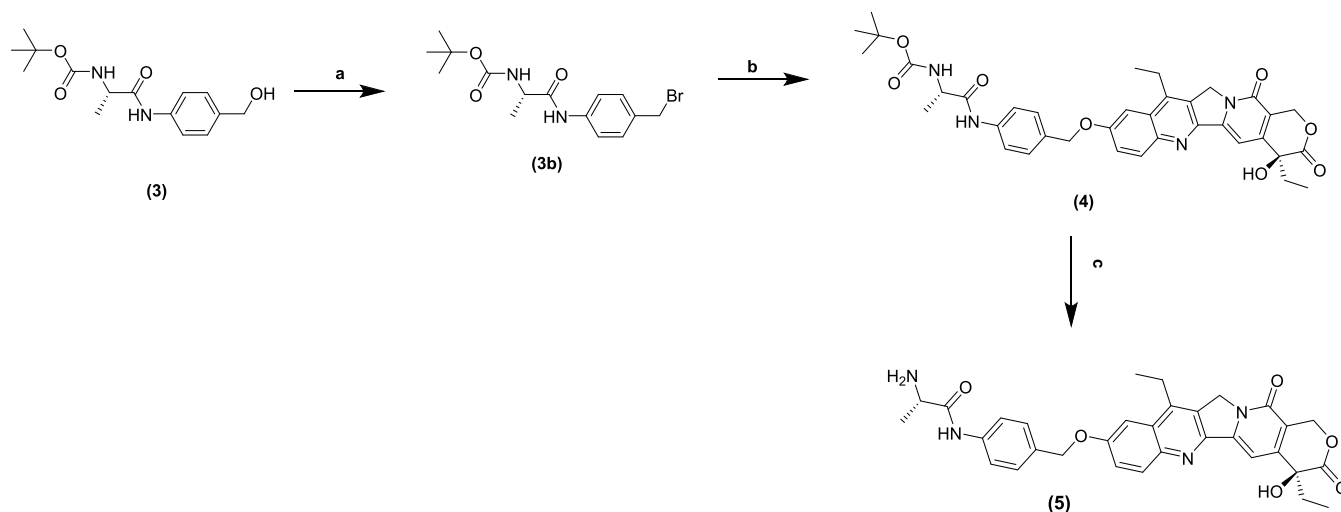**Figure 3.** Structure of the T7-PEG$_4$-N$_3$ targeting peptide (**1**).

Figure 4. Structure of DBCO-PEG$_3$-Ahx-Val (**2**).

Scheme 1. Synthetic Route for the Preparation of NH$_2$-Ala-PAB-SN-38[a]

[a]Reagents and conditions: All reactions were performed at room temperature unless otherwise noted. (a) Phosphorus tribromide (PBr3), tetrahydrofuran/dichloromethane (50:50), 3 h. (b) SN-38, 18-crown-6, potassium carbonate, dimethylformamide, 40 °C, 3 h. (c) 20% trifluoroacetic acid in dichloromethane, 2 h.

isomers of the peptides were generated with the built-in ConfGen algorithm. Following the ligand processing, SiteMap was deployed to identify possible peptide binding sites and the druggability of each site. A SiteScore is generated, which takes into consideration factors such as (a) the size of the site, (b) how solvent-exposed the site is, (c) the degree of enclosure of the protein, (d) the hydrophobic and hydrophilic nature of the site, (e) the proximity of the site point interaction with the protein (i.e., tightness of interaction), and (f) the degree of h-bond donor and acceptor interaction. The larger the SiteScore, the more druggable a site is, so the docking site was selected based on the overall score and the site size, considering the large size of the peptide. In addition, we cross-referenced the selected site with that reported in the T7 docking studies on TfR conducted by Tang et al.[26] Thus, the centroid of the docking grid was positioned between the key binding residues (E244, E266, E533, and E714). The receptor grid for peptide

docking was generated using Maestro's Receptor Grid Generation tool. The center of the grid box was supplied as a coordinate ($[x, y, z] = [3, -70, 13]$) upon adjustment to incorporate the entire peptide within the receptor grid. The ligand was docked into the receptor grid with standard precision (SP-Peptide) with Epik state penalties for pose predictions and glide scoring.

Synthesis of T7-PEG$_4$-N$_3$ (1). N$_3$-PEG$_4$-His-Ala-Ile-Tyr-Pro-Arg-His (**1**) (Figure 3) was synthesized using a modified published method.[46] Solid-phase peptide synthesis (SPPS) was employed by utilizing the standard Fmoc protocol. Briefly, H-His (Trt)-2-Cl-Trt resin (3.25g, 2.6 mmol) was swollen in DMF for 2 h. The sequence of protected amino acids was introduced in the following order: Fmoc-L-Arg(Pbf)-OH, Fmoc-L-Pro-OH, Fmoc-L-Tyr(tBu)-OH, Fmoc-L-Ile-OH, Fmoc-L-Ala-OH, and Fmoc-L-His(tBu)-OH. All couplings were conducted in DMF using 2.5 equiv of each amino acid
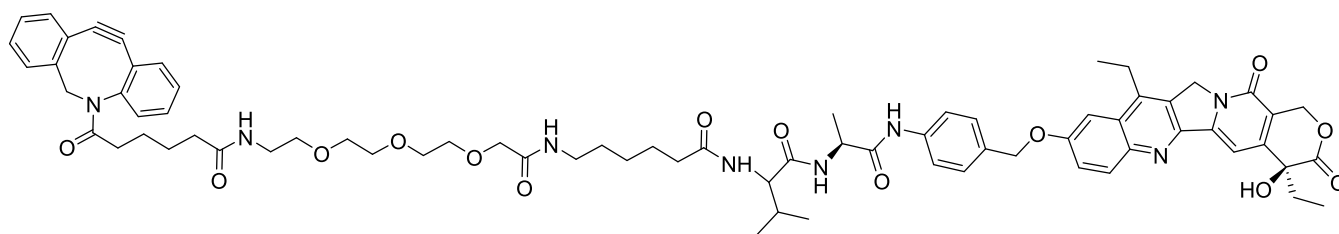
Figure 5. Structure of DBCO-PEG$_3$-AHX-Val-Ala-PAB-SN-38 (**6**).

and 5 equiv of DIPEA. HATU (2.45 equiv) was used as a coupling agent, with each coupling cycle lasting for 1 h (Supporting Information, Scheme 1). After each coupling, the Fmoc protecting group was removed using a solution of 20% piperidine in DMF. Following the coupling of the final amino acid, the N-terminus of the peptide was capped using an azide-terminated polyethylene glycol linker (N$_3$-PEG$_4$-acid). Following the reaction, the peptidyl resin was washed sequentially with DMF, DCM, and then with methanol. The peptidyl resin was dried under vacuum overnight. T7-PEG$_4$-N$_3$ (**1**) was cleaved from the polymeric support using a TFA/TIPS/H$_2$O cocktail (95:2.5:2.5) and concentrated under vacuum. The concentrate was precipitated in ether, and the product was obtained as a yellow crystalline solid (3.5 g, 86%). Compound 1 was characterized by analytical HPLC and ESI-MS. The compound was used without further purification. ESI m/z 1166.99; ([C$_{52}$H$_{79}$N$_{17}$O$_{14}$+H]$^+$ calcd. 1166.61) (Supporting Information, Figure 1). Analytical HPLC revealed a single peak with a retention time (RT) of 4.97 min, showing that the compound is pure (Supporting Information, Figure 2).

Synthesis of DBCO-PEG$_3$-Ahx-Val (2). DBCO-PEG$_3$-Ahx-Val (**2**) (Figure 4) was synthesized using a modified published method.[46] Briefly, H-Val-2-Cl-Trt resin (7.5 g, 4.9 mmol/g) was swollen in DMF for 2 h. After swelling, Fmoc-6-aminohexanoic acid (2.5 equiv), Fmoc-N-amido-PEG$_3$-acid (1.5 equiv), and DBCO-C$_6$-acid (1.5 equiv) were coupled successively. All couplings were conducted in DMF with 5 equiv of DIPEA and HATU (2.45 equiv), with each coupling cycle lasting for 1 h. DBCO-PEG$_3$-Ahx-Val (**2**) was cleaved from the resin with 1% TFA in DCM and concentrated by rotary evaporation. The concentrated product was precipitated in cold diethyl ether and dried under vacuum (Supporting Information, Scheme 2). The product was obtained as a dark-colored viscous liquid (4.25 g, 84%), characterized using ESI-MS, and used without further purification. ESI m/z 735.26; ([C$_{40}$H$_{54}$N$_4$O$_9$+H]$^+$ calcd. 735.40) (Supporting Information, Figure 4).

Synthesis of Boc-Ala-PABA (3). To a solution of Boc-ala-OH (8.00 g, 42.2 mmol) in dry acetonitrile were added EEDQ (13.59 g, 54.9 mmol) and 4-aminobenzyl alcohol (PABA) (6.77 g, 54.9 mmol) dissolved in 15 mL of anhydrous DMF (Scheme 1). The resulting solution was stirred at room temperature for 15 h, and the progress of the reaction was monitored by thin-layer chromatography (TLC) and mass spectrometry (ESI-MS). The final product was purified using silica gel column chromatography (70−230 mesh) (ethyl acetate/hexane 35/65) to yield Boc-Ala-PABA (**3**) (8.89 g, 71%). ^{1}H NMR (400 MHz, CDCl$_3$) δ 9.69 (s, 1H), 7.84 (d, J = 8.0 Hz, 2H), 7.76 (s, 1H), 7.59 (d, J = 8.0 Hz, 2H), 6.09 (s, 1H), 5.06 (m, 1H), 4.93 (s, 1H), 1.94 (s, 9H), 1.78 (d, J = 6.0 Hz, 1H). ESI-MS m/z 295.17; ([C$_{15}$H$_{22}$N$_2$O$_4$+H]$^+$ calcd..295.17) (Supporting Information, Figure 5 (ESI-MS

spectrum) and Figure 7 (^{1}H NMR spectrum)). Analytical HPLC revealed a single peak with a retention time (RT) of 4.96 min, showing that the compound is pure RT (Supporting Information, Figure 6).

Synthesis of Boc-Ala-PAB-SN-38 (4). To a solution of Boc-Ala-PABA (**3**) (3.5 g, 11.8 mmol) in dry THF (20 mL) on an ice bath was slowly added phosphorus tribromide (PBr$_3$) (3.2 g, 11.8 mmol) in anhydrous DCM (20 mL).[47] The progress of the reaction was monitored by TLC. After 3 h, the reaction was complete, and the solution was transferred into cold water (250 mL). The dichloromethane layer was collected through multiple extractions and dried by using anhydrous sodium sulfate (Scheme 1). After evaporation of the solvent under vacuum, the crude solid product compound **3b** was obtained (1.45 g, 41%). Compound **3b** was used without further purification.

To a solution of SN-38 (0.58 g, 1.47 mmol) in anhydrous DMF (60 mL) was added potassium carbonate (0.307 g, 2.24 mmol) and 18-crown-6 (0.058 g, 10 mol %) at room temperature for 15 min (Scheme 1).[48] A bright orange solution was observed. Compound **3b** (0.8 g, 2.24 mmol) was added to the reaction, and the temperature was set to 40 °C. After the mixture was stirred for 3 h, the reaction was stopped, and the reaction flask was placed in a refrigerator for 1 h to precipitate the solid potassium carbonate, followed by filtration to remove insoluble solid materials. The crude product obtained by evaporation of the filtrate was purified using preparatory HPLC. Boc-Ala-PAB-SN-38 (**4**) was obtained as a yellow powder (0.45 g, 46%). ^{1}H NMR (400 MHz, DMSO) δ 10.01 (s, 1H), 8.09 (d, J = 9.2 Hz, 1H), 7.96 (s, 1H), 7.65 (d, J = 8.5 Hz, 2H), 7.57 (d, J = 9.4 Hz, 1H), 7.27 (s, 1H), 7.11 (d, J = 7.3 Hz, 1H), 5.43 (s, 2H), 5.31 (s, 2H), 4.11 (s, 1H), 3.19 (d, J = 8.2 Hz, 2H), 2.89 (s, 5H), 1.38 (s, 9H). ESI-MS m/z 669.16; ([C$_{37}$H$_{40}$N$_4$O$_8$+H]$^+$ calcd. 669.29) (Supporting Information, (Figure 8 ESI-MS spectrum) and Figure 10 (^{1}H NMR spectrum)). Analytical HPLC revealed a single peak with RT of 7.04 min, showing that the compound is pure (Supporting Information, Figure 9).

Synthesis of NH$_2$-Ala-PAB-SN-38 (5). Boc-Ala-PAB-SN-38 (**4**) (0.45 g, 0.672 mmol) was dissolved in 20% TFA in dichloromethane to initiate Boc deprotection.[47] The mixture was stirred at room temperature for 2 h and monitored via TLC (Scheme 1). The crude product was obtained by evaporation. NH$_2$-Ala-PAB-SN-38 (**5**) was obtained as a yellow powder and used without further purification (0.30grams,78%.) ^{1}H NMR (400 MHz, DMSO) δ 10.47 (s, 1H), 8.17 (s, 4H), 8.10 (d, J = 9.1 Hz, 1H), 7.95 (s, 1H), 7.66−7.45 (m, 5H), 7.27 (s, 1H), 5.43 (s, 2H), 5.31 (d, 4H), 3.99 (s, 1H). ESI-MS m/z 569.27; ([C$_{32}$H$_{32}$N$_4$O$_6$ + H]$^+$ calcd. 569.24) (Supporting Information, Figure 11 (ESI-MS) and Figure 13 (^{1}H NMR)). Analytical HPLC revealed a single peak
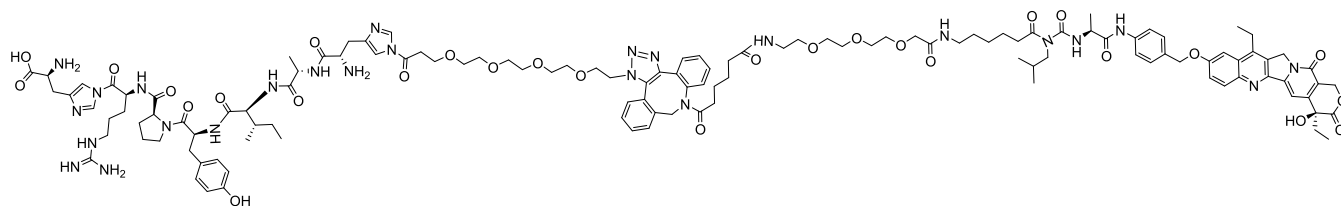
Figure 6. Structure of T7-SN-38-targeted drug conjugate (**7**).

with RT of 4.88 min, showing that the compound is pure (Supporting Information, Figure 12)

*Synthesis of DBCO-PEG₃-Ahx-Val-Ala-PAB-SN-38 (**6**).* DBCO-PEG₃-Ahx-Val (**2**) and NH₂-Ala-PAB-SN-38 (**5**) were coupled together in a simple amide bond formation step using HATU as a coupling reagent.[49] To a solution of DBCO-PEG₃-Ahx-Val (**2**) (0.27 g, 0.350 mmol) in anhydrous DMF was added HATU (0.065 g, 0.343 mmol) and DIPEA (0.24 mL, 0.14 mmol). After activation of the carboxyl group for 15 min, NH₂-Ala-PAB-SN-38 (**5**) (0.2 g, 0.350 mmol) was added, and the progress of the reaction was monitored using analytical HPLC. After 3 h, the organic solvent was evaporated, and the final product was purified by preparatory HPLC (Figure 5). DBCO-PEG₃-Ahx-Val-Ala-PAB-SN-38 was obtained as a yellow solid (0.125 g, 28.40%). Analytical HPLC revealed a single peak with RT of 7.13 min, showing that the compound is pure (Supporting Information, Figure 14). ESI *m/z* 1285.997; ([$C_{72}H_{84}N_8O_{14}$+H])⁺calcd.1285.62 (Supporting Information, Figure 15).

*Strain-Promoted Azide-Alkyne Cycloaddition (SPAAC) (**7**).* T7-PEG₄-N₃ (**1**) (0.06 g, 0.058 mmol) and DBCO-PEG₃-Ahx-Val-Ala-PAB-SN-38 (**6**) (0.05 g, 0.038 mmol) were dissolved in anhydrous DMF. The vial was clamped to a fixed-angle tube rotator, rotated at 10 rpm, and maintained at 37 °C for 24 h. The reaction was purified using preparative HPLC, and the synthesis of the targeted drug conjugate was confirmed by ESI-MS. T7-SN-38, the targeted drug conjugate (**7**) (Figure 6), was obtained as a yellow viscous oil (0.032 g, 34%). ESI *m/z* 2454.40; M/2 1227.42; and M/3 818.34 (Supporting Information, Figure 16). Analytical HPLC revealed a single peak with an RT of 5.17 min, showing that the compound is pure (Supporting Information, Figure 17).

In Vitro **Cleavage Studies of T7-SN-38 by Cathepsin.** The following protocols were modified to evaluate the cleavage profile of T7-SN-38 (**7**):[50−52] 11 μL of cathepsin B (human liver, 0.47 mg/mL, 324U/mg) (Merck Millipore, Merck GA) stock was added to 27.2 μL of activation buffer (30 mM DTT, 15 mM EDTA in H₂O) and incubated for 15 min at room temperature. The mixture was diluted with 4.9 mL of reaction buffer (150 mM sodium acetate buffer, 12 mM EDTA, 24 mM DTT, in H₂O; pH 6.0), and the reaction was initiated with the addition of 70 μL of a stock solution of the T7-SN-38 drug conjugate (**7**) in DMSO (final conjugate concentration: 183 μM). The mixture was incubated at 37 °C. Aliquots were withdrawn at predetermined time intervals, and cleavage was assessed by RP-HPLC as a function of time from 0−24 h. The HPLC chromatogram peak areas at the characteristic RT of pure drug and conjugate were used to determine both the disappearance of the T7-SN-38 conjugate as well as the appearance of free SN-38. As a control, the study was performed in the absence of cathepsin B under similar conditions as described above.

Evaluation of the Stability of the T7-Targeted SN-38 Peptide Drug Conjugate. The T7-SN-38 conjugate (**7**) was dissolved in 2.5 mL of phosphate buffer saline (PBS) (pH 7.4) containing 2% DMSO at a final conjugate concentration of 196 μM and incubated at 37 °C per modified published procedures.[50,53] Aliquots of the mixture were withdrawn at different time points (0−24 h) and analyzed by HPLC.

Cell Culture. Human glioma cell lines U87MG were purchased from the American Type Culture Collection (ATCC). The cells were grown and maintained in Eagle's minimum essential medium (EMEM) supplemented with 10% FBS (Corning, Manassas, VA) and 1% penicillin−streptomycin (Sigma-Aldrich) at 37 °C in an incubator with a 5% CO₂ atmosphere.

Cytotoxicity Assay. U87MG cells were seeded in 96-well plates at a density of 1×10^4 cells/well. At 24 h, the cultured cells were treated with SN-38 or T7-SN-38 conjugate at various concentrations (from 5 nM to 160 nM) and incubated at 37 °C. At 24 and 72 h, 70 μL of 2,3-bis-(2-methoxy-4-nitro-5-sulfophenyl)-2H-tetrazolium-5-carboxanilide (XTT reagent mixed with an electron coupling reagent) solution was added to each well. After 3 h of incubation, the absorbance was measured at 450 nm using a Biotek ELx808 absorbance microplate reader (Lonza, Walkersville, MD). The absorbance values were normalized to the control group (cells without treatment), and percent cell viability was plotted using GraphPad Prism 10 (GraphPad Software, Inc.). The XTT assay is a colorimetric method used to assess cell viability and proliferation by measuring the metabolic activity of cells based on their ability to reduce a tetrazolium salt (XTT) to a soluble formazan dye. The results are represented as the mean ± standard deviation of four replicates (*n* = 4).

T7 Competition Assay: Transferrin Receptor Blocking Studies. U87MG (1×10^4) cells were seeded in 96-well plates. After 24 h, the media was replaced with media containing a 10-fold molar excess of T7-PEG₄-N₃ relative to the T7-SN-38 conjugate and incubated for 1 h. After 1h incubation, the cells were treated with SN-38 or T7-SN-38 at various concentrations (from 5 to 160 nM). Cells treated with DMSO (0.05%) and media-only treated cells served as controls. The experiment was repeated, and an XTT assay was performed at 72 h for the 72 h viability evaluations. The percent cell viability based on absorbance at 450 nm was calculated relative to controls. The results are represented as the mean ± std of four replicates (*n* = 4).

T7 Competition Assay: Exogenous Cathepsin B Studies. U87MG cells at a density of 1×10^4 were initially plated into 96-well plates and allowed to incubate for 24 h to facilitate cell adhesion. Following this incubation period, the culture medium was replaced with media containing a 10-fold molar excess of T7-PEG₄-N₃ relative to the conjugate, and the cells were incubated for 1h. Subsequently, the cells were treated either with 80 nM SN-38 or T7-SN-38 conjugate
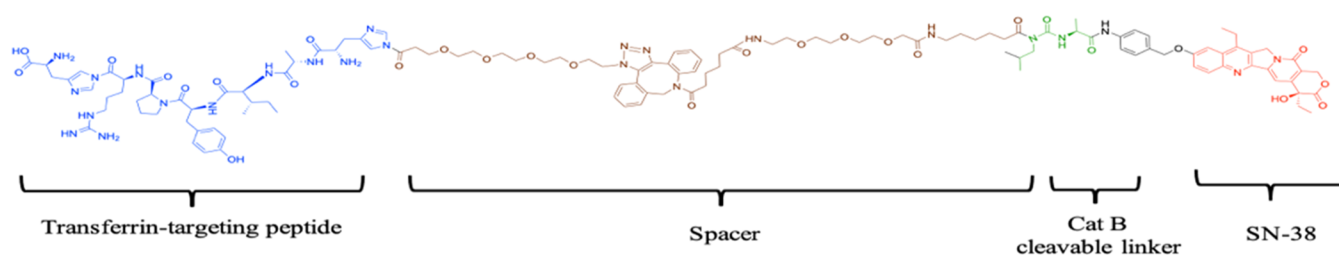
Figure 7. Structure of the peptide drug conjugate T7-SN-38. T7-SN-38 contains a transferrin targeting peptide, a spacer, a Cat B cleavable substrate, a self-immolative linker (PABA), and SN-38.
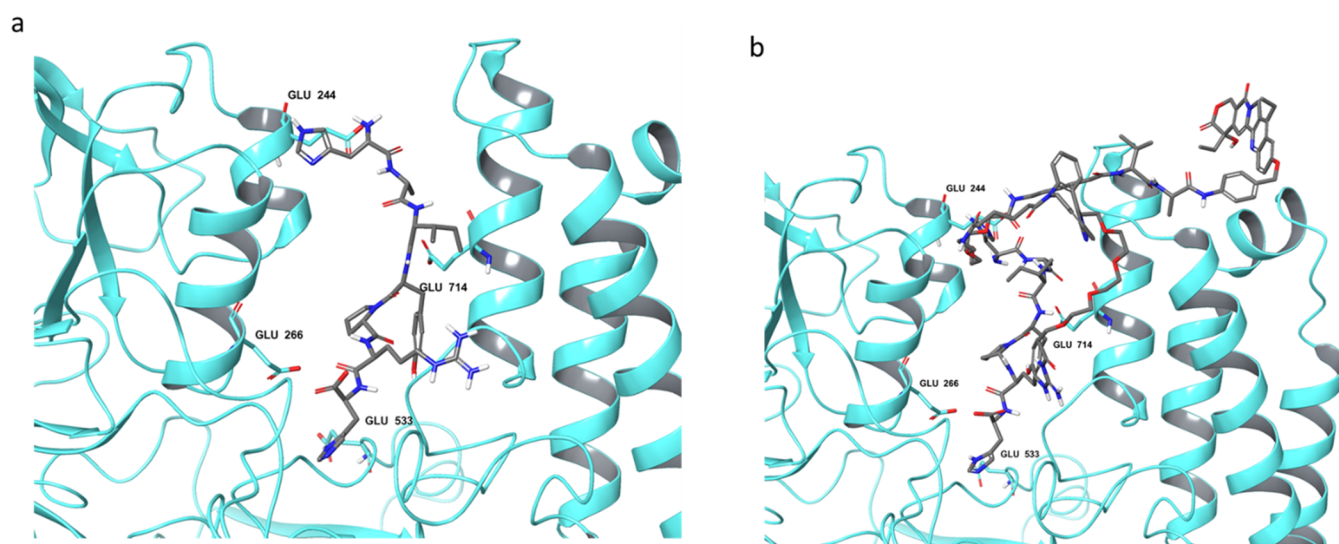

Figure 8. Results of Glide docking predicted protein-peptide poses. (a) T7 peptide in gray, bound to TfR, the cyan 2D protein structure, with a Glide score of −9.950 kcal/mol. (b) T7-SN-38 peptide conjugate in gray, bound to TfR, the cyan 2D protein structure, with a Glide score of − 5.543 kcal/mol.

containing 80 nM SN-38 and were coincubated with exogenous cathepsin B. In a parallel experiment, cells that were initially exposed to excess T7-PEG$_4$-N$_3$ were then treated with 80 nM SN-38 or T7-SN-38 without the addition of exogenous cathepsin B. The XTT assay was performed at 72 h per manufacturer protocol, and the data was used for viability calculations. The percent cell viability data was plotted using GraphPad Prism 10. The results are represented as the mean ± std of four replicates ($n = 4$).

Statistical Analysis. Data are presented as the mean ± standard deviation (SD) unless otherwise indicated. The IC$_{50}$ values were calculated by fitting a concentration−response curve using Microsoft Excel 16.77 (Microsoft Corporation, CA). The difference between any two groups was determined by ANOVA. $P < 0.05$ was considered statistically significant.

■ RESULTS

Design of the T7 Peptide Drug Conjugate. The synthesized peptide drug conjugate consists of five distinct components: (i) a transferrin receptor targeting peptide (HAIYPRH); (ii) spacer; (iii) a VA peptide sequence susceptible to cleavage by cathepsin B; (iv) a self-immolative linker (PABA); and (v) the cytotoxic agent (SN-38) (Figure 7). By design, T7-SN-38 is expected to selectively bind to transferrin receptors that are expressed on the surface of the BBB because of the T7 peptide affinity for TfR. Once bound, it is transported via receptor-mediated transcytosis across the BBB into the brain parenchyma, where it encounters and binds

to glioblastoma cells, which has been reported to overexpress the TfR about 100-fold higher compared to healthy cells. Binding to glioblastoma cells leads to cellular uptake and Cat B-mediated cleavage, followed by self-immolation by 1,6 elimination to release free, active drug resulting in specific cytotoxicity to cancer cells.

Molecular Docking Study. We report the predicted pose and predicted binding affinity of T7 peptide compared with those of T7-SN-38 from which we can infer the possibility of binding to TfR by both the free peptide and conjugate. The molecular docking study demonstrates superior binding of the T7 peptide, with predicted glide scores (i.e., binding affinity) ranging from −10.234 to −9.950 kcal/mol (Figure 8a). T7 makes multiple favorable H-bonds within the TfR binding site, as well as a salt-bridge interaction with Glu244. On the other hand, T7-SN-38 exhibited lower predicted binding affinity due to its larger size and increased torsional flexibility, with the best score of −5.543 kcal/mol, which is less than a 2-fold difference in score. However, the T7 sequence of both the peptide and conjugate are oriented similarly in the target site of TfR, with the penultimate Arg-His of both oriented toward Glu533 and the remainder of the peptide elongated along the helical domain. In Figure 8b, SN-38 extends into the solvent-accessible region and does not make much interaction with the protein, thereby providing easy accessibility of protease to hydrolyze and cleave at the Cat B cleavable peptide site.

Synthesis of the T7-Targeted SN-38 Peptide Drug Conjugate (T7-SN-38). Boc-Ala-PABA (**3**) was conjugated to
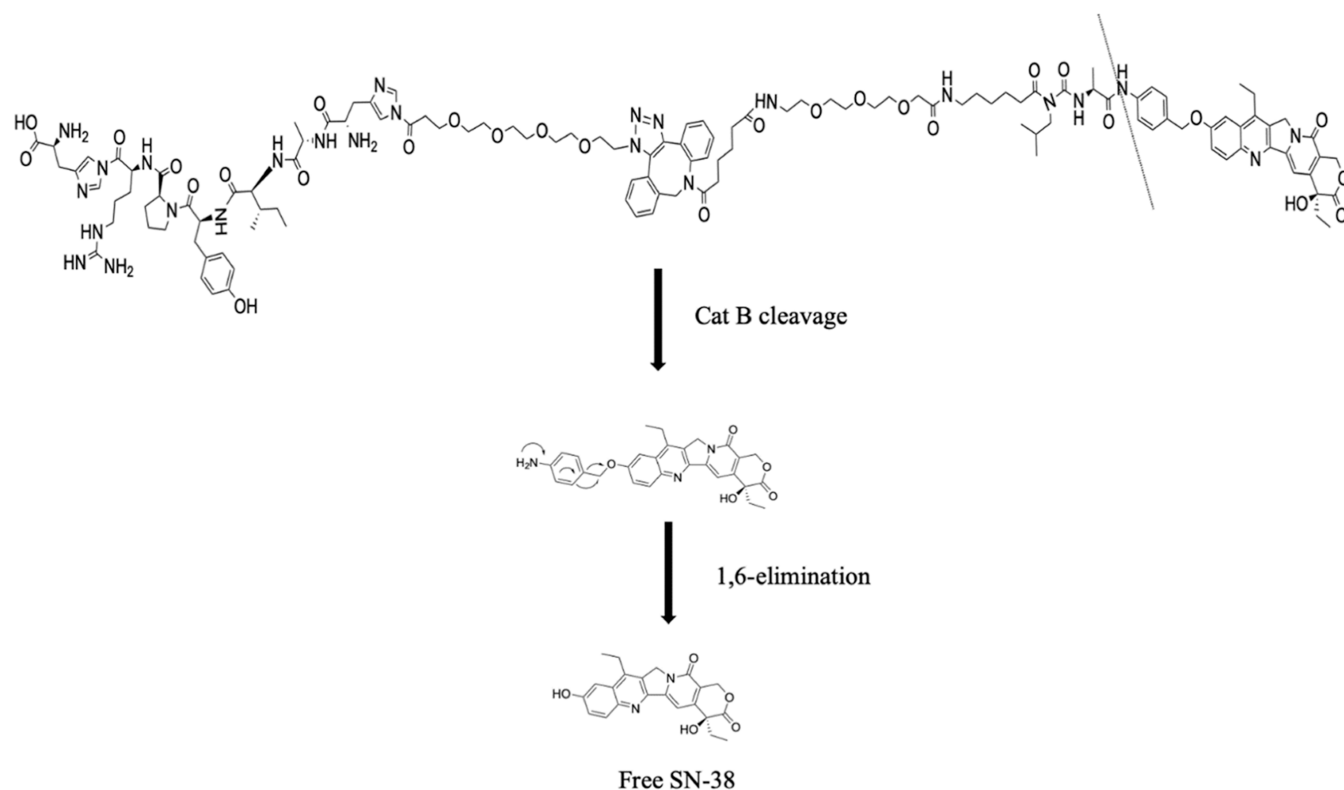
Figure 9. Proposed cleavage mechanism of T7-SN-38 to release SN-38.

the hydroxyl group (C-10-OH) on SN-38 via a stable ether bond (Scheme 1). DBCO-PEG₃-Ahx-Val (**2**) was coupled to NH₂-Ala-PAB-SN-38 (**5**) obtained after the Boc deprotection of Boc-Ala-PAB-SN-38 (**4**). For the synthesis of the T7-SN-38 conjugate, peptide T7 was synthesized by SPPS (Supporting Information, Scheme 2) and terminated with PEG₄-azide. Synthesis of N₃-PEG₄-HAIYPRH was confirmed with mass spectrometry (m/z = 1166.99) (Supporting Information, Figure S1). FT-IR spectroscopy data show a peak at 2100 cm⁻¹, confirming the presence of the azide functional group (Supporting Information, Figure S3). The reaction between N₃-PEG₄-HAIYPRH and DBCO-PEG₃-Ahx-Val-Ala-PAB-SN-38 was allowed to continue in DMF for 24 h at 37 °C to improve yield. The conjugate was purified using preparative HPLC and characterized by analytical HPLC for purity (Figure S17) and mass spectrometry (Figure S16).

In Vitro Cleavage Studies of T7-SN-38 by Cathepsin B. The release of the parent drug (SN-38) from the T7-SN-38 conjugate is essential to eliciting cytotoxicity in glioblastoma cells. We hypothesize that T7-SN-38 would be delivered to the glioblastoma cells and cleaved by cathepsin B to release free SN-38 (Figure 9). To investigate the release of SN-38 by enzymatic cleavage, exogenous cathepsin B was added to solutions of the conjugate, and aliquots of the resulting solution were withdrawn at different times and analyzed by analytical HPLC over 24 h. Results obtained by HPLC show that approximately 80% of the T7-SN-38 conjugate was cleaved by Cat B to release free SN-38 (Figure 10), with the appearance of peaks consistent with the retention time of the parent drug (RT = 4.8 min), and the drug conjugate (RT = 5.2 min) (Supporting Information, Figure S18). Over time, the area of the peak at the RT of the conjugate decreased while that of the parent drug increased. Subsequently, the
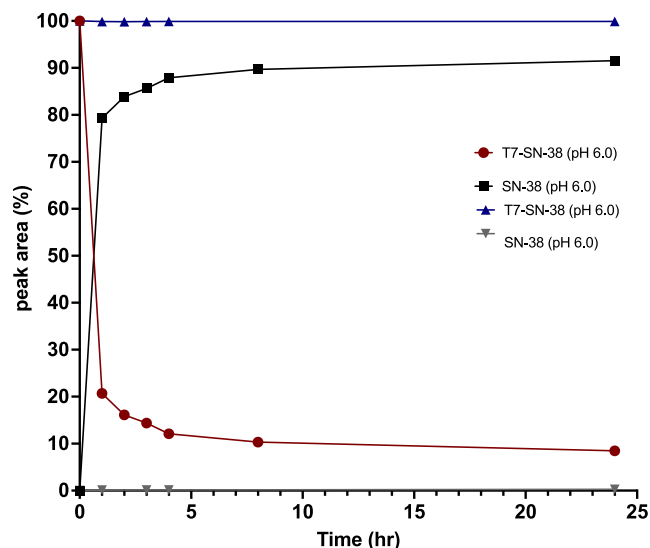
Figure 10. Cleavage studies data showing the area plot of the conjugate solution in the presence of cathepsin B (T7-SN-38; red line), appearance of the parent drug (SN-38; black line), the control conjugate solution in the absence of exogenous cathepsin B (T7-SN-38; blue line), and appearance of free SN-38 in the absence of cathepsin B (T7-SN-38; gray line) (n = 3).

identification of the cleavage products was achieved by mass spectrometry. The results showed that SN-38 (m/z = 393.47) was released from the T7-SN-38 conjugate (m/z = 2454.40; m/2 = 1226.61) in the presence of Cat B (Supporting Information, Figure S19). The T7-SN-38 conjugate was almost fully degraded within 24 h. No free SN-38 was observed when the conjugate was incubated in enzyme free buffer at pH (6.0) for 24 h (Figure 11).

Figure 11. Stability studies data showing the area plot of T7-SN-38 stability in PBS (pH 7.4; red line) and the appearance of free SN-38 (pH 7.4; black line) ($n = 3$).

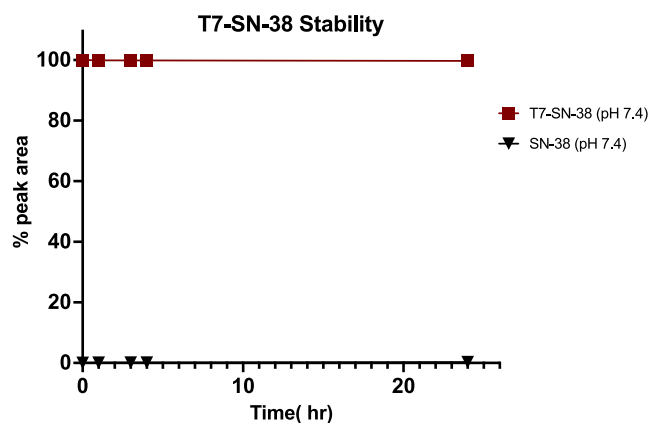**Stability Measurements of the T7-Targeted SN-38 Peptide Drug Conjugate.** The stability of the T7-targeted peptide drug conjugate was analyzed in phosphate-buffered saline (pH 7.4) at 37 °C for 24 h to simulate the pH of the blood (Figure 11). There was no change in the pattern and retention time (RT = 5.142 min) of the conjugate peak at different time points when analyzed by HPLC (Supporting Information, Figure S20), indicating that the conjugate was stable and that there was very minimal decomposition or cleavage of the conjugate at physiological pH.

Cell Culture Experiments. *T7-SN-38 Cytotoxicity against U87MG Glioblastoma Cell Lines.* The cytotoxicity of SN-38 and T7-SN-38 (containing the same equivalent of SN-38) on U87MG cells over a range of concentrations was evaluated. Results show that within the range of concentrations tested, both T7-SN-38 and SN-38 did not exert pronounced cytotoxicity at 24 h (Figure 12a). SN-38 showed significantly more cytotoxic activity when compared with the conjugate ($p < 0.05$). In addition, a concentration-dependent effect on the viability of U87MG was observed with both treatments. Over a 72 h period, however, both T7-SN-38 and SN-38 demon-

strated considerable cytotoxicity on U87MG cells. Like the data obtained at 24 h, a concentration-dependent effect was observed within the range of concentrations evaluated. Additionally, a time-dependent increase in cytotoxicity was observed when the 72 h data was compared with 24 h data. Furthermore, since a 0.05% DMSO solution was used to dissolve the test agents and prepare stock solutions, the effect of DMSO on cell viability at the maximum concentration used was evaluated. Results show similar viability with media-treated cells and lack of toxicity (Figure 12b). Further, IC_{50} values of SN-38 and T7-SN-38 on U87MG cells at 72 h were determined. An estimated IC_{50} value of 26.41 nM was obtained for SN-38, which was considerably lower than an IC_{50} value of 70.07 nM obtained for the T7-SN-38 conjugate. These IC_{50} data confirm the greater cytotoxicity of the pure drug compared to the conjugate at 72 h ($p < 0.05$).

T7 Competition Assay: Transferrin Receptor Blocking Studies. To determine whether the cytotoxicity of T7-SN-38 is facilitated by receptor-mediated endocytosis as hypothesized, U87MG cells seeded in 96-well plates were treated with excess N_3-PEG_4-T7 for 1 h (blocking) prior to treatment with either SN-38 or T7-SN-38. Initial evaluations confirmed that treatment of U87MG cells with 10x of T7 peptide was not cytotoxic (data not shown). Although transferrin receptors were blocked, concentration-dependent cytotoxicity was observed in U87MG cells treated with free SN-38 for 24 and 72 h (Figure 13a,b). The calculated IC_{50} at 72 h was 27.63 nM (Figure 13b). In contrast, U87MG cells treated with T7-SN-38 did not show an appreciable reduction in cell viability at 24 and 72 h. Approximately 80% cell viability was observed in cells treated with high nanomolar concentrations of T7-SN-38 (containing the same equivalent of free SN-38) at 72 h, compared with <30% viability observed in cells treated with similar concentrations of free drug (Figure 13b). This experiment suggests that the developed peptide drug conjugate (PDC) binds to transferrin receptors on cultured U87MG cells to facilitate endocytosis, followed by intracellular Cat B cleavage to release free cytotoxic SN-38. Once this mechanism is blocked, cytotoxicity is not observed. However, since SN-38 acts independently of the transferrin receptor, it caused a
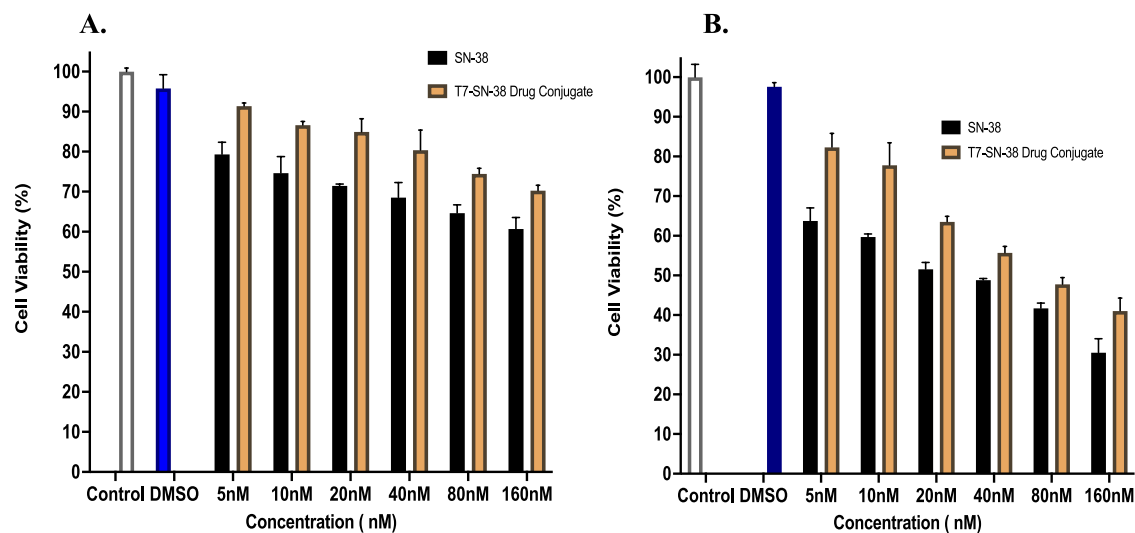

Figure 12. Percent viability data showing the effect of SN-38 and the T7-SN-38 conjugate on U87MG cell lines after 24 h exposure to treatment (a) and after 72 h exposure to treatment (b). Controls represent 0.05% DMSO in medium and growth medium only. The results are represented as the mean ± std ($n = 4$).
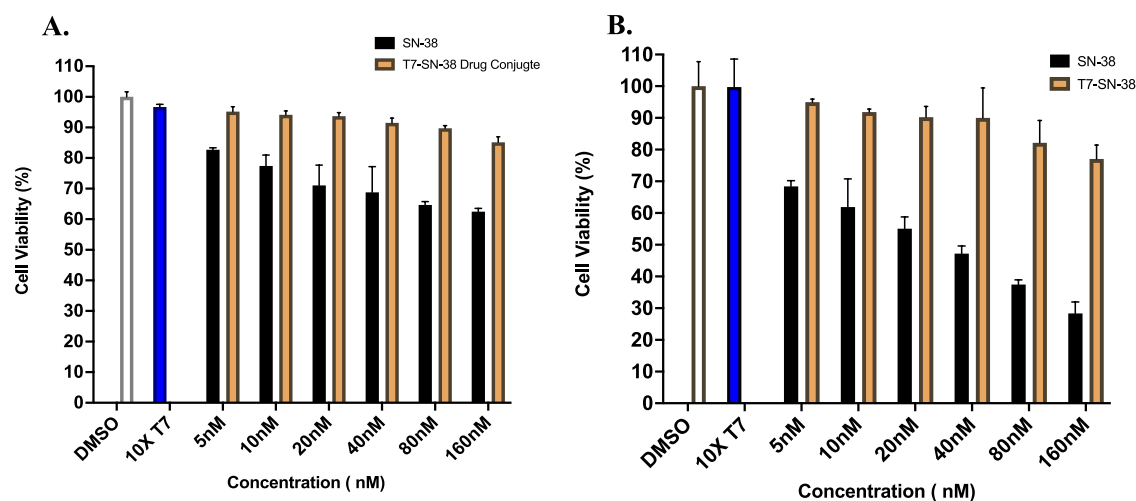
Figure 13. Percent cell viability data showing the effect of SN-38 and T7-SN-38 on U87MG cell lines after (a) 24 h exposure to treatment in TfR-blocked cells and (b) 72 h exposure to treatment in TfR-blocked cells. Media, 0.05% DMSO solution in medium, and cells blocked with a 10-fold molar excess of the T7 peptide served as controls. The results are represented as the mean $\pm$ std ($n = 4$).

significant decrease ($p < 0.05$) in cell viability and an increase in cell death, regardless of whether the receptors were blocked or not blocked with N_3-PEG_4-T7.

T7 Competition Assay: Validation of Importance of the Transferrin Receptor for Observed Cytotoxicity. To validate whether the cytotoxicity of the synthesized conjugate relied on receptor-mediated endocytosis and enzymatic cleavage for drug release, the transferrin receptors on U87MG cells were blocked with excess targeting peptide, as described above. The cells with blocked transferrin receptors were treated with culture media containing 80 nM SN-38 and T7-SN-38 containing the equivalent of 80 nM SN-38, and culture media containing exogenous cathepsin B in addition to 80 nM SN-38 and T7-SN-38 containing the equivalent of 80 nM SN-38. As depicted in Figure 14, cells with blocked transferrin receptors treated with the conjugate did not exhibit an appreciable decrease in cell viability at 72 h. In contrast, SN-38 demonstrated potent cytotoxicity in free drug-treated cells. Interestingly, when targeted conjugate-treated cells with blocked transferrin receptors were exposed to media containing exogenous cathepsin B, a notable increase in cell death was observed. Collectively, these outcomes establish that the effectiveness of our developed drug conjugate indeed hinges on its binding with transferrin receptors, followed by internalization and exposure to intracellular cathepsin B and subsequent enzymatic cleavage of the conjugate to release the active drug, which then prompts a cytotoxic response.

◼ DISCUSSION

Glioblastoma (GBM) is classified as an incurable and malignant form of cancer.[55] As our understanding of GBM's molecular biology continues to expand, emerging areas such as tumor proliferation, angiogenesis, cell migration, and the ability to penetrate the blood−brain barrier are providing novel prospects for the advancement of GBM treatments.[56] Transferrin receptors (TfR) play a vital role in glioblastoma by facilitating iron uptake, supporting cell growth, and potentially serving as targets for therapeutic interventions and diagnostic applications. The expression of TfR on the BBB and its overexpression on glioblastoma cells makes them important molecular targets for advancing glioblastoma research and
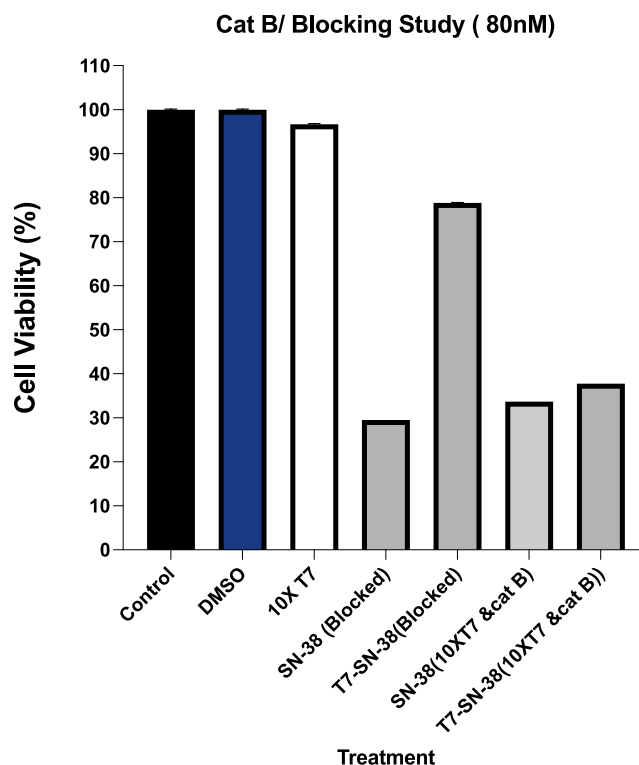
Figure 14. Percent cell viability data in U87MG cells preincubated with excess T7 targeting ligand and treated with culture media containing 80 nM SN-38 and T7-SN-38 containing 80 nM SN-38; and culture media containing exogenous cathepsin B in addition to 80 nM SN-38 and T7-SN-38 containing 80 nM SN-38 after 72 h exposure to treatment. Control wells are media only, 0.05% DMSO in medium and 10-fold molar excess of the T7 peptide. The. The results are represented as the mean $\pm$ std ($n = 4$).

treatment strategies.[57,58] Several researchers have reported that targeting transferrin receptors allows for the selective delivery of therapeutic agents to glioblastoma cells while sparing healthy brain tissue. In agreement with this observation, the T7 peptide has been researched for brain targeting, to improve biodistribution, and to improve the efficacy of drugs in the treatment of glioblastoma.[13,55] T7 peptide targeting of the TfR

can potentially minimize adverse effects associated with conventional glioblastoma chemotherapy treatments that affect both cancerous and normal cells; thus, the T7 peptide was selected for use as a targeting ligand for site-specific SN-38 delivery in this work. To evaluate the suitability of the peptide for targeting and as proof of the strategy, molecular docking analysis[54] of the T7-SN-38 chemical structure reveals that the conjugate fits into the T7 binding site on the TfR; however, its larger size reduces its binding affinity despite adopting a similar orientation within the target site as the free targeting ligand. However, the coupled SN-38 does not exhibit substantial interaction with the binding region and extends into a solvent-accessible region, thereby allowing protease accessibility to hydrolyze and cleave at the Cat B cleavable peptide site. To confirm this, the conjugate was designed, and T7-SN-38 was successfully synthesized and characterized.

In this study, we have successfully showcased a strategy involving the conjugation of SN-38 to the T7 peptide through a valine-alanine Cat B recognition sequence. This approach holds the potential to significantly enhance the delivery of SN-38 to glioblastoma by leveraging the binding affinity of T7 peptide to the TfR expressed on the BBB and overexpressed on glioma cells. Subsequently, the conjugate undergoes intracellular Cat B-mediated cleavage, enabling site-specific payload delivery to glioblastoma cells. Cat B is overexpressed in glioblastoma cells, making it a suitable target for selectively directing therapeutic interventions.[32,59]

Using this strategy, the 10-OH position of SN-38 was modified to establish a stable ether linkage between SN-38 and the T7 peptide using a Cat B labile linker as the mechanism of drug release. This crucial requirement of the hydrolytic stability of the conjugate in circulation is pivotal to the drug delivery strategy.

By conjugation of SN-38 to the Cat B linker, the SN-38 payload can be released specifically within tumor cells. This approach holds the potential to minimize off-target effects, leading to better treatment outcomes and reduced side effects. In addition, reports have shown that in SN-38, the 10-OH position is available for enzymatic glucuronidation in vivo. Thus, coupling at the 10-OH position inhibits glucuronidation, thereby protecting the 10-OH and ensuring T7-SN-38 stability under physiological conditions until intracellular localization in tumor cells and release of free SN-38.[60,61]

In the context of an SN-38 ether-based drug delivery system, data from stability studies at pH 7.4 show that the structural integrity of the conjugate is maintained within the period evaluated. This is similar to literature reports.[47,62] These data suggest that the conjugate could be stable to degradation while in circulation. This stability is essential to prevent premature drug release, which could lead to unintended toxic effects on healthy cells. Moreover, as confirmed in Figure 12, the conjugation of SN-38 to the hydroxyl group delays activity until cleavage by Cat B, followed by 1,6 elimination to release the free drug. Data from in vitro cleavage studies reveal that incubation of the conjugate with Cat B led to a significant decrease in the peak area of the conjugate within 1 h, with complete cleavage observed by 24 h when analyzed by HPLC. This observation underscores the pivotal role of the cathepsin B-sensitive linker as the mechanism of SN-38 release. Furthermore, in vitro cleavage studies not only validated the enzymatic cleavage of T7-SN-38 but also demonstrated the lack of cleavage and stability of the conjugate in the absence of cathepsin B in control experiments at pH 6. Our approach has

great translational potential and may present an innovative therapeutic approach.

Biological evaluation of the synthesized targeted conjugate was carried out in vitro using a cell-based model of glioblastoma. U87MG is a malignant glioma cell line that endogenously overexpresses the TfR.[63] The cytotoxicity of the SN-38-containing conjugate, free SN-38, and other controls in U87MG cells were studied using the XTT assay. The data show the concentration- and time-dependent effect of the drug and conjugate on the viability of U87MG cells. As the concentrations of both SN-38 and the conjugate increase, the viability decreases, consistent with the potent cytotoxic nature of SN-38. In addition, as the duration of treatment increases from 24 to 72 h, cell viability decreases. This data is consistent with several published literature on the time-dependent cytotoxicity of SN-38 in several anticancer efficacy studies in different cell lines.[36,64,65]

To assess the specificity of the drug conjugate for the transferrin receptor, to relate receptor-mediated uptake to cytotoxic efficacy, and to determine the differences (if any) in the uptake mechanism of free SN-38 and targeted SN-38 conjugate, transferrin receptor blocking studies were carried out. Competition for binding to the transferrin receptor was ensured by pretreatment of the cells with a 10-fold excess of the targeting ligand for 1 h before treatment with the targeted SN-38 conjugate and pure SN-38 as the control, followed by assessment of cytotoxicity. Our data reveal that the cytotoxicity of the T7-targeted conjugate was significantly inhibited when compared to the cytotoxicity of the free drug, which was largely uninhibited (Figure 11). The difference in the observed cytotoxicity could be explained by the mechanism of the internalization of the two agents. It is expected that free SN-38 diffuses into the cell by passive diffusion to elicit its effects; thus, the blockade of the transferrin receptor is not expected to inhibit the cytotoxicity of free SN-38. However, with the transferrin receptor-targeted SN-38 conjugate, competition between excess free T7 targeting ligand and the T7-targeted SN-38 conjugate may explain the inhibition of uptake by receptor-mediated endocytosis with the attendant lack of toxicity since uptake via the transferrin receptor must precede intracellular cleavage and release of the free cytotoxic SN-38.

Another series of experiments was carried out to assess the specificity and importance of enzymatic conjugate cleavage to cytotoxicity, confirm the role of transferrin receptor—ligand interactions in uptake and, thereby, therapeutic efficacy, and validate the importance of the transferrin receptor for targeted therapy. In these studies, U87MG cells pretreated with the free T7 targeting ligand for 1 h were treated with T7-SN-38 containing 80 nM equivalent of SN-38 and 80 nM of SN-38, to which exogenous Cat B was added. Control experiments were carried out without exogenous Cat B (Figure 12). Despite the blockade of the TfR as a result of preincubation with the free targeting ligand, cells treated with T7-SN-38 in the presence of exogenous cathepsin B exhibited considerable cytotoxicity after 72 h, similar to the cytotoxic effect observed with free drug (Figure 12). These results validate the desirability and importance of the critical design attributes built into the design and construction of the targeted SN-38 delivery system. It validates the importance of intracellular localization for cathepsin B cleavage and efficient drug release, which is assured by T7-mediated binding to overexpressed transferrin receptors on the cell surface. The results validate the proposed

approach for T7 peptide-targeted therapy in the treatment of glioblastoma.

CONCLUSIONS

A transferrin receptor-targeted SN-38 conjugate (T7-SN-38) was successfully synthesized to deliver SN-38 across the blood−brain barrier and selectively into glioblastoma cells using transferrin receptors expressed on the BBB surface and overexpressed on the surface of glioblastoma cells. This innovative strategy shows demonstrable cellular uptake in U87MG cells, as evaluated in several biological experiments. Furthermore, the protease activity of intracellular Cat B cleaves the peptide drug conjugate, releasing the active drug to elicit toxicity in cancer cells. We postulate that after the initial interaction between T7-SN-38 and the TfR located on the cell surface, the receptor−ligand complex undergoes internalization via the process of receptor-mediated endocytosis. This internalization facilitates the enzymatic conjugate cleavage and release of the free drug within glioblastoma cells mediated by intracellular cathepsin B, leading to site-specific cytotoxicity. Our results highlight the promising translational potential of the delivery strategy as a site-specific therapeutic approach for individuals with brain cancer. Our findings strongly suggest that T7-SN-38 holds considerable promise as a chemotherapeutic strategy for treating glioblastoma and warrants further in-depth investigation. Work is ongoing to evaluate the reported strategy for the T7-targeted combination delivery of a PARP inhibitor and SN-38 to the brain for the treatment of glioblastoma. These conjugates were evaluated in vivo in subsequent studies.

ASSOCIATED CONTENT

Supporting Information

The Supporting Information is available free of charge at https://pubs.acs.org/doi/10.1021/acsomega.3c07486.

Additional experimental details, such as synthetic schemes of peptides via SPPS, ESI-MS spectra of all synthesized compounds, ^{1}H NMR spectra for select compounds, analytical HPLC spectra for synthesized peptides and conjugates, and FT-IR spectra of select compounds (PDF)

AUTHOR INFORMATION

Corresponding Author

Simeon K. Adesina − Department of Pharmaceutical Sciences, Howard University, Washington D.C. 20059, United States; orcid.org/0000-0002-9841-9971; Phone: 202-250-5304; Email: simeon.adesina@howard.edu; Fax: 202-806-7805

Authors

Perpetue Bataille Backer − Department of Pharmaceutical Sciences, Howard University, Washington D.C. 20059, United States

Tayo Alex Adekiya − Department of Pharmaceutical Sciences, Howard University, Washington D.C. 20059, United States

Yushin Kim − Department of Pharmaceutical Sciences, Concordia University of Wisconsin, Mequon, Wisconsin 53097-2402, United States

Terry-Elinor R. Reid − Department of Pharmaceutical Sciences, Concordia University of Wisconsin, Mequon, Wisconsin 53097-2402, United States

Michael Thomas − Department of Biology, Howard University, Washington D.C. 20059, United States

Complete contact information is available at:
https://pubs.acs.org/10.1021/acsomega.3c07486

Notes

The authors declare no competing financial interest.

REFERENCES

(1) Cho, C. F.; Farquhar, C. E.; Fadzen, C. M.; et al. A Tumor-Homing Peptide Platform Enhances Drug Solubility, Improves Blood−Brain Barrier Permeability and Targets Glioblastoma. *Cancers* **2022**, *14* (9), 2207.

(2) Pineda, E.; Domenech, M.; Hernández, A.; Comas, S.; Balaña, C. Recurrent Glioblastoma: Ongoing Clinical Challenges and Future Prospects. *OncoTargets Ther.* **2023**, *Volume 16*, 71−86.

(3) Yeini, E.; Ofek, P.; Albeck, N.; et al. Targeting Glioblastoma: Advances in Drug Delivery and Novel Therapeutic Approaches. *Adv Ther.* **2021**, *4* (1), No. 2000124.

(4) Janjua, T. I.; Rewatkar, P.; Ahmed-Cox, A.; et al. Frontiers in the treatment of glioblastoma: Past, present and emerging. *Adv. Drug Delivery Rev.* **2021**, *171*, 108−138.

(5) Ferraris, C.; Cavalli, R.; Panciani, P. P.; Battaglia, L. Overcoming the Blood−Brain Barrier: Successes and Challenges in Developing Nanoparticle-Mediated Drug Delivery Systems for the Treatment of Brain Tumours. *Int. J. Nanomed.* **2020**, *15*, 2999−3022.

(6) Zhang, F.; Xu, C. L.; Liu, C. M. Drug delivery strategies to enhance the permeability of the blood brain barrier for treatment of glioma. *Drug Des Devel. Ther.* **2015**, 2089−2100.

(7) Yang, K.; Wu, Z.; Zhang, H.; et al. Glioma targeted therapy: insight into future of molecular approaches. *Mol. Cancer* **2022**, *21* (1), 39.

(8) van Tellingen, O.; Yetkin-Arik, B.; De Gooijer, M. C.; Wesseling, P.; Wurdinger, T.; De Vries, H. E. Overcoming the blood−brain tumor barrier for effective glioblastoma treatment. *Drug Resistance Updates* **2015**, *19*, 1−12.

(9) Choudhury, H.; Pandey, M.; Chin, P. X.; et al. Transferrin receptors-targeting nanocarriers for efficient targeted delivery and transcytosis of drugs into the brain tumors: a review of recent advancements and emerging trends. *Drug Delivery Transl. Res.* **2018**, *8* (5), 1545−1563.

(10) Aldape, K.; Brindle, K. M.; Chesler, L.; et al. Challenges to curing primary brain tumours. *Nat. Rev. Clin. Oncol.* **2019**, *16* (8), 509−520.

(11) D'Alessio, A.; Proietti, G.; Sica, G.; Scicchitano, B. M. Pathological and Molecular Features of Glioblastoma and Its Peritumoral Tissue. *Cancers* **2019**, *11* (4), 469.

(12) Meng, J.; Agrahari, V.; Youm, I. Advances in Targeted Drug Delivery Approaches for the Central Nervous System Tumors: The Inspiration of Nanobiotechnology. *J. Neuroimmune Pharmacol.* **2017**, *12* (1), 84−98.

(13) Pulgar, V. M. Transcytosis to Cross the Blood Brain Barrier, New Advancements and Challenges. *Front. Neurosci.* **2019**, *12*, 1019.

(14) Johnsen, K. B.; Burkhart, A.; Melander, F.; et al. Targeting transferrin receptors at the blood-brain barrier improves the uptake of immunoliposomes and subsequent cargo transport into the brain parenchyma. *Sci Rep.* **2017**, *7* (1), No. 10396.

(15) Li, J.; Zheng, M.; Shimoni, O.; et al. Development of Novel Therapeutics Targeting the Blood−Brain Barrier: From Barrier to Carrier. *Adv. Sci.* **2021**, *8* (16), No. 2101090.

(16) Ayloo, S.; Gu, C. Transcytosis at the blood−brain barrier. *Curr. Opin. Neurobiol.* **2019**, *57*, 32−38.

(17) Kuang, Y.; An, S.; Guo, Y.; et al. T7 peptide-functionalized nanoparticles utilizing RNA interference for glioma dual targeting. *Int. J. Pharm.* **2013**, *454* (1), 11−20.

(18) Ramalho, M. J.; Loureiro, J. A.; Coelho, M. A. N.; Pereira, M. C. Transferrin Receptor-Targeted Nanocarriers: Overcoming Barriers to Treat Glioblastoma. *Pharmaceutics* **2022**, *14* (2), 279.

(19) Arvanitis, C. D.; Ferraro, G. B.; Jain, R. K. The blood−brain barrier and blood−tumour barrier in brain tumours and metastases. *Nat. Rev. Cancer* **2020**, *20* (1), 26−41.

(20) Wang, S.; Meng, Y.; Li, C.; Qian, M.; Huang, R. Receptor-Mediated Drug Delivery Systems Targeting to Glioma. *Nanomaterials* **2016**, *6* (1), 3.

(21) Papademetriou, I. T.; Porter, T. Promising approaches to circumvent the blood−brain barrier: progress, pitfalls and clinical prospects in brain cancer. *Ther Delivery* **2015**, *6* (8), 989−1016.

(22) Bi, Y.; Liu, L.; Lu, Y.; et al. T7 Peptide-Functionalized PEG-PLGA Micelles Loaded with Carmustine for Targeting Therapy of Glioma. *ACS Appl. Mater. Interfaces* **2016**, *8* (41), 27465−27473.

(23) Cheng, X.; Yu, D.; Cheng, G.; et al. T7 Peptide-Conjugated Lipid Nanoparticles for Dual Modulation of Bcl-2 and Akt-1 in Lung and Cervical Carcinomas. *Mol. Pharmaceutics* **2018**, *15* (10), 4722−4732.

(24) Cui, L.; Wang, Y.; Liang, M.; et al. Dual-modified natural high density lipoprotein particles for systemic glioma-targeting drug delivery. *Drug Delivery* **2018**, *25* (1), 1865−1876.

(25) Zong, T.; Mei, L.; Gao, H.; et al. Enhanced Glioma Targeting and Penetration by Dual-Targeting Liposome Co-modified with T7 and TAT. *J. Pharm. Sci.* **2014**, *103* (12), 3891−3901.

(26) Tang, J.; Wang, Q.; Yu, Q.; et al. A stabilized retro-inverso peptide ligand of transferrin receptor for enhanced liposome-based hepatocellular carcinoma-targeted drug delivery. *Acta Biomater.* **2019**, *83*, 379−389.

(27) Mckertish, C.; Kayser, V. Advances and Limitations of Antibody Drug Conjugates for Cancer. *Biomedicines* **2021**, *9* (8), 872.

(28) Wang, Y.; Cheetham, A. G.; Angacian, G.; Su, H.; Xie, L.; Cui, H. Peptide−drug conjugates as effective prodrug strategies for targeted delivery. *Adv. Drug Delivery Rev.* **2017**, *110−111*, 112−126.

(29) Hoppenz, P.; Els-Heindl, S.; Beck-Sickinger, A. G. Peptide-Drug Conjugates and Their Targets in Advanced Cancer Therapies. *Front. Chem.* **2020**, *8*, 571.

(30) Chavda, V. P.; Solanki, H. K.; Davidson, M.; Apostolopoulos, V.; Bojarska, J. Peptide-Drug Conjugates: A New Hope for Cancer Management. *Molecules* **2022**, *27* (21), 7232.

(31) Bargh, J. D.; Isidro-Llobet, A.; Parker, J. S.; Spring, D. R. Cleavable linkers in antibody−drug conjugates. *Chem. Soc. Rev.* **2019**, *48* (16), 4361−4374.

(32) Rao, J. S. Molecular mechanisms of glioma invasiveness: the role of proteases. *Nat. Rev. Cancer* **2003**, *3* (7), 489−501.

(33) Aggarwal, N.; Sloane, B. F. Cathepsin B: Multiple roles in cancer. *Proteomics: Clin. Appl.* **2014**, *8* (5−6), 427−437.

(34) Yanamandra, N.; Gumidyala, K. V.; Waldron, K. G.; et al. Blockade of cathepsin B expression in human glioblastoma cells is associated with suppression of angiogenesis. *Oncogene* **2004**, *23* (12), 2224−2230.

(35) Wang, Y.; Fan, S.; Zhong, W.; Zhou, X.; Li, S. Development and Properties of Valine-Alanine based Antibody-Drug Conjugates with Monomethyl Auristatin E as the Potent Payload. *Int. J. Mol. Sci.* **2017**, *18* (9), 1860.

(36) Jin, X.; Zhang, J.; Jin, X.; Liu, L.; Tian, X. Folate Receptor Targeting and Cathepsin B-Sensitive Drug Delivery System for Selective Cancer Cell Death and Imaging. *ACS Med. Chem. Lett.* **2020**, *11* (8), 1514−1520.

(37) Wu, Z.; Li, S.; Cai, Y.; Chen, F.; Chen, Y.; Luo, X. Synergistic action of doxorubicin and 7-Ethyl-10-hydroxycamptothecin poly-phosphorylcholine polymer prodrug. *Colloids Surf., B* **2020**, *189*, No. 110741.

(38) Obidiro, O.; Battogtokh, G.; Akala, E. O. Triple Negative Breast Cancer Treatment Options and Limitations: Future Outlook. *Pharmaceutics* **2023**, *15* (7), 1796.

(39) Dai, Y.; Qian, M.; Li, Y. Structural Modification Endows Small-Molecular SN38 Derivatives with Multifaceted Functions. *Molecules* **2023**, *28* (13), 4931.

(40) Li, Y.; Xie, M.; Jones, J. B.; et al. Targeted Delivery of DNA Topoisomerase Inhibitor SN38 to Intracranial Tumors of Glioblastoma Using Sub-5 Ultrafine Iron Oxide Nanoparticles. *Adv. Healthcare Mater.* **2022**, *11* (14), No. 2102816.

(41) Manaspon, C.; Nasongkla, N.; Chaimongkolnukul, K.; et al. Injectable SN-38-loaded Polymeric Depots for Cancer Chemotherapy of Glioblastoma Multiforme. *Pharm. Res.* **2016**, *33* (12), 2891−2903.

(42) Palakurthi, S. Challenges in SN38 drug delivery: current success and future directions. *Expert Opin. Drug Delivery* **2015**, *12* (12), 1911−1921.

(43) Eckenroth, B. E.; Steere, A. N.; Chasteen, N. D.; Everse, S. J.; Mason, A. B. How the binding of human transferrin primes the transferrin receptor potentiating iron release at endosomal pH. *Proc. Natl. Acad. Sci. U.S.A.* **2011**, *108* (32), 13089−13094.

(44) Tubert-Brohman, I.; Sherman, W.; Repasky, M.; Beuming, T. Improved Docking of Polypeptides with Glide. *J. Chem. Inf. Model* **2013**, *53* (7), 1689−1699.

(45) Madhavi Sastry, G.; Adzhigirey, M.; Day, T.; Annabhimoju, R.; Sherman, W. Protein and ligand preparation: parameters, protocols, and influence on virtual screening enrichments. *J. Comput. Aided Mol. Des.* **2013**, *27* (3), 221−234.

(46) Coin, I.; Beyermann, M.; Bienert, M. Solid-phase peptide synthesis: from standard procedures to the synthesis of difficult sequences. *Nat. Protoc.* **2007**, *2* (12), 3247−3256.

(47) Liu, L.; Xie, F.; Xiao, D.; et al. Synthesis and evaluation of highly releasable and structurally stable antibody-SN-38-conjugates. *Drug Delivery* **2021**, *28* (1), 2603−2617.

(48) António, J. P. M.; Carvalho, J. I.; André, A. S.; et al. Diazaborines Are a Versatile Platform to Develop ROS-Responsive Antibody Drug Conjugates**. *Angew Chem Int. Ed.* **2021**, *60* (49), 25914−25921.

(49) Vrettos, E. I.; Sayyad, N.; Mavrogiannaki, E. M.; et al. Unveiling and tackling guanidinium peptide coupling reagent side reactions towards the development of peptide-drug conjugates. *RSC Adv.* **2017**, *7* (80), 50519−50526.

(50) Karnthaler-Benbakka, C.; Koblmüller, B.; Mathuber, M.; et al. Synthesis, Characterization and *in vitro* Studies of a Cathepsin B-Cleavable Prodrug of the VEGFR Inhibitor Sunitinib. *Chem. Biodiversity* **2019**, *16* (1), No. e1800520.

(51) Dubowchik, G. M.; Firestone, R. A.; Padilla, L.; et al. Cathepsin B-Labile Dipeptide Linkers for Lysosomal Release of Doxorubicin from Internalizing Immunoconjugates: Model Studies of Enzymatic Drug Release and Antigen-Specific In Vitro Anticancer Activity. *Bioconjugate Chem.* **2002**, *13* (4), 855−869.

(52) Taha, T. A.; El-Alwani, M.; Hannun, Y. A.; Obeid, L. M. Sphingosine kinase-1 is cleaved by cathepsin B in vitro: Identification of the initial cleavage sites for the protease. *FEBS Lett.* **2006**, *580* (26), 6047−6054.

(53) Tai, W.; Shukla, R. S.; Qin, B.; Li, B.; Cheng, K. Development of a Peptide−Drug Conjugate for Prostate Cancer Therapy. *Mol. Pharmaceutics* **2011**, *8* (3), 901−912.

(54) Meng, X. Y.; Zhang, H. X.; Mezei, M.; Cui, M. Molecular Docking: A Powerful Approach for Structure-Based Drug Discovery. *Curr. Comput. Aided-Drug Des.* **2011**, *7* (2), 146−157.

(55) Davis, M. Glioblastoma: Overview of Disease and Treatment. *Clin. J. Oncol. Nursing* **2016**, *20* (5), S2−S8.

(56) Dymova, M. A.; Kuligina, E. V.; Richter, V. A. Molecular Mechanisms of Drug Resistance in Glioblastoma. *Int. J. Mol. Sci.* **2021**, *22* (12), 6385.

(57) Daniels, T. R.; Bernabeu, E.; Rodríguez, J. A.; et al. The transferrin receptor and the targeted delivery of therapeutic agents against cancer. *Biochim. Biophys. Acta, Gen. Subj.* **2012**, *1820* (3), 291−317.

(58) Ramalho, M. J.; Loureiro, J. A.; Coelho, M. A. N.; Pereira, M. C. Transferrin Receptor-Targeted Nanocarriers: Overcoming Barriers to Treat Glioblastoma. *Pharmaceutics* **2022**, *14* (2), 279.

(59) Demchik, L. L.; Sameni, M.; Nelson, K.; Mikkelsen, T.; Sloane, B. F. Cathepsin B and glioma invasion. *Int. J. Dev. Neurosci.* **1999**, *17* (5−6), 483−494.

(60) Goldenberg, D. M.; Sharkey, R. M. Antibody-drug conjugates targeting TROP-2 and incorporating SN-38: A case study of anti-TROP-2 sacituzumab govitecan. *mAbs* **2019**, *11* (6), 987−995.

(61) Whang, C. H.; Yoo, E.; Hur, S. K.; Kim, K. S.; Kim, D.; Jo, S. A highly GSH-sensitive SN-38 prodrug with an "OFF-to-ON" fluorescence switch as a bifunctional anticancer agent. *Chem Commun.* **2018**, *54* (65), 9031−9034.

(62) Lau, U. Y.; Benoit, L. T.; Stevens, N. S.; et al. Lactone Stabilization is Not a Necessary Feature for Antibody Conjugates of Camptothecins. *Mol. Pharmaceutics* **2018**, *15* (9), 4063−4072.

(63) Koneru, T.; McCord, E.; Pawar, S.; Tatiparti, K.; Sau, S.; Iyer, A. K. Transferrin: Biology and Use in Receptor-Targeted Nano-therapy of Gliomas. *ACS Omega* **2021**, *6* (13), 8727−8733.

(64) Wu, C.; Zhang, Y.; Yang, D.; et al. Novel SN38 derivative-based liposome as anticancer prodrug: an in vitro and in vivo study. *Int. J. Nanomed.* **2019**, *Volume 14*, 75−85.

(65) Huang, Q.; Liu, X.; Wang, H.; et al. A nanotherapeutic strategy to overcome chemoresistance to irinotecan/7-ethyl-10-hydroxy-camptothecin in colorectal cancer. *Acta Biomater.* **2022**, *137*, 262−275.